

3. PHASE TRANSITIONS, TWINNING AND DOMAIN STRUCTURES

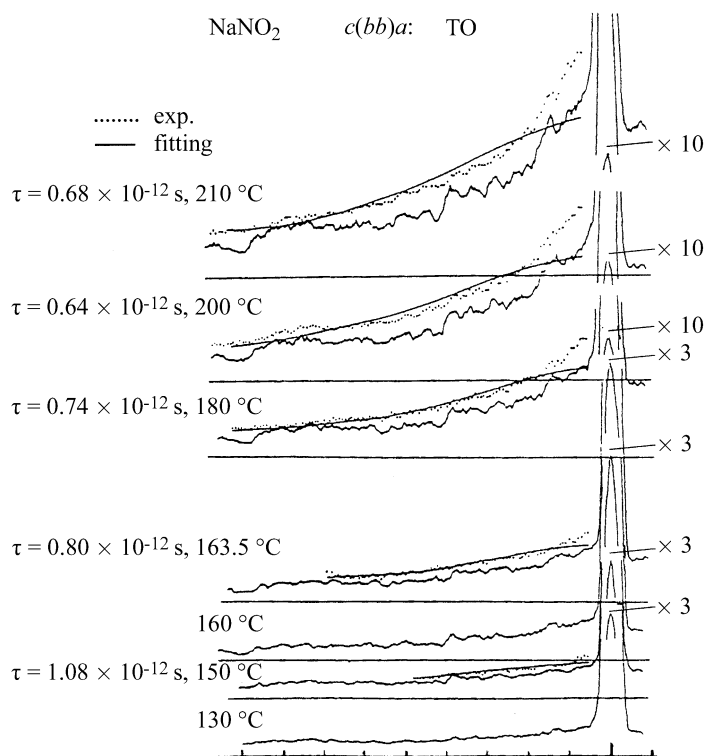


Fig. 3.1.5.20. Raman spectra of sodium nitrite, showing diffusive Debye-like response due to large-amplitude flopping over of nitrite ions [note that the high-frequency phonon-like response is due to the small-amplitude motion of this same normal mode; thus in this system N ions give rise not to $3N$ (non-degenerate) peaks in the spectral response function, but to $3N + 1$].

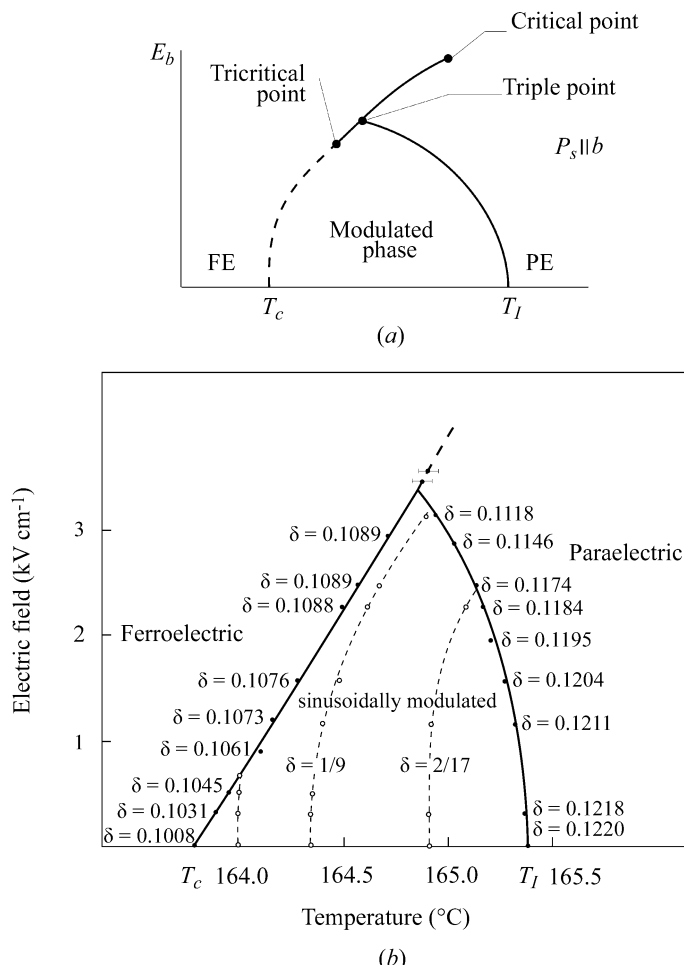


Fig. 3.1.5.21. Phase diagram for sodium nitrite for ‘conjugate’ electric fields applied along the polar b axis, showing triple point, tricritical point and critical end point. (a) Schematic; (b) real system.

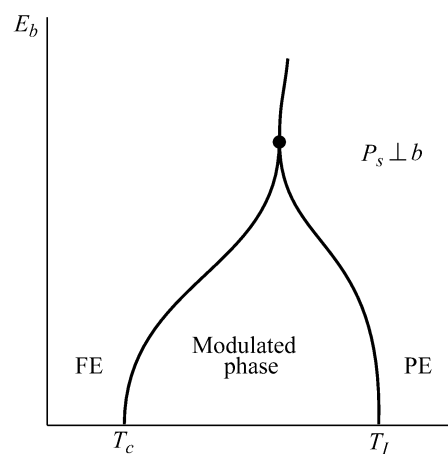


Fig. 3.1.5.22. Phase diagram for sodium nitrite for electric fields applied perpendicular to the polar b axis. In this situation, a Lifshitz point is possible where phase boundaries ‘kiss’ (touch tangentially).

polar axis. As Fig. 3.1.5.21 illustrates somewhat schematically, there are first-order phase boundaries, second-order phase boundaries, a tricritical point and a critical end point (as in a gas–liquid diagram). If the electric field is applied in a direction orthogonal to the polar axis, a Lifshitz point (Fig. 3.1.5.22) may be expected, in which the phase boundaries intersect tangentially. The ionic conductivity of sodium nitrite has made it difficult to make the figures in Figs. 3.1.5.21 and 3.1.5.22 precise.

3.1.5.2.12. Fast ion conductors

As exemplary of this class of materials, we discuss in this section the silver iodide compound $\text{Ag}_{13}\text{I}_9\text{W}_2\text{O}_8$. This material has the structure illustrated in Fig. 3.1.5.23. Conduction is *via* transport of silver ions through the channels produced by the W_2O_{16} ions (the coordination is not that of a simple tetrahedrally coordinated WO_4 tungstate lattice).

This crystal undergoes three structural phase transitions (Habbel *et al.*, 1978; Greer *et al.*, 1980; Habbel *et al.*, 1980), as illustrated in Fig. 3.1.5.24. The two at lower temperatures are first-order; that at the highest temperature appears to be perfectly continuous. Geller *et al.* (1980) tried to fit electrical data for this material ignoring the uppermost transition.

As in most of the materials discussed in this review, the phase transitions were most readily observed *via* optical techniques, Raman spectroscopy in particular. The subtle distortions involve oxygen positions primarily and are not particularly well suited to more conventional X-ray techniques. Silver-ion disorder sets in only above the uppermost phase transition, as indicated by the full spectral response (as in the discussion of sodium nitrite in the preceding section).

Infrared (Volkov *et al.*, 1985) and Raman (Shawabkeh & Scott, 1989) spectroscopy have similarly confirmed low-temperature phase transitions in RbAg_4I_5 at 44 and 30 K, in addition to the well studied D_3^7 – D_3^2 ($R32$ – $P321$) transition at 122 K. The two lower-temperature phases increase the size of the primitive cell, but their space groups cannot be determined from available optical data. The 44 K transition is signalled by the abrupt appearance of an intense phonon feature at 12 cm^{-1} in both infrared and Raman spectra.

3.1.5.2.13. High-temperature superconductors

It is useful to play Devil’s Advocate and point out difficulties with the technique discussed, to indicate where caution might be exercised in its application. $\text{YBa}_2\text{Cu}_3\text{O}_{7-x}$ (YBaCuO) provides such a case. As in the case of BaMnF_4 discussed in Section 3.1.5.2.7, there was strong evidence for a structural phase transition near 235 K, first from ultrasonic attenuation (Wang, 1987;